Sensors and Materials, Vol. 35, No. 8 (2023) 2817–2829
MYU Tokyo

S & M 3357

Analyses of Full-load, Modal, and Fatigue Life of Electric Motorcycle Frame Using Finite Element Software ANSYS

Hong-Mei Dai,[1] Bo-Hao Chen,[2] Chao-Ming Hsu,[2*]
Chiang-Lung Lin,[1] and Cheng-Fu Yang[3,4**]

[1]College of Art, Zhongqiao Vocational and Technical University, Shanghai 201514, China
[2]Department of Mechanical Engineering, National Kaohsiung University of Science and Technology, Kaohsiung 807, Taiwan
[3]Department of Chemical and Materials Engineering, National University of Kaohsiung, Kaohsiung 811, Taiwan
[4]Department of Aeronautical Engineering, Chaoyang University of Technology, Taichung 413, Taiwan

(Received April 18, 2023; accepted July 5, 2023)

Keywords: analysis and design, single layer, reticulated, ANSYS Workbench, dome

There are two methods of analyzing the effects of various loads on the full-load, modal, and fatigue life of an electric motorcycle frame. The first method involves attaching stress sensors to the frame, and the second method utilizes finite element method (FEM) software for simulation. In this study, the simulation method was employed, and this paper details the creation of an analysis system for an electric motorcycle frame using FEM software tools such as Visual Basic and ANSYS parametric design languages. By inputting geometric models and parameters, the system generated LOG files to create FEM models of the motorcycle frame. These LOG files were then imported into ANSYS for structural analysis, which included full-load analysis, modal analysis, and fatigue life analysis. By utilizing the aforementioned models, users were able to easily perform full-load, modal, and fatigue life analyses of the electric motorcycle frame by inputting the necessary parameters into function tables. During the full-load analysis, various forces were applied at different positions to determine the maximum stress, deformation, and strain values. The modal analysis of the electric motorcycle frame involved determining the first through sixth orders of the natural vibration frequencies and modes (mode shape), as well as the vibration frequencies and modes under full load. In the fatigue life analysis, a fatigue tool was used to apply forces ranging from 50 to 200% of the full-load boundary condition. Additionally, the relationship between the number of cycles to failure (N) and the applied stress amplitude was examined.

1. Introduction

In recent years, there has been a steady rise in global carbon emissions, leading to an intensified greenhouse effect and more frequent extreme climate-related events. This increase in carbon emissions not only impacts the global climate but also leads to severe air pollution.

*Corresponding author: e-mail: jammy@nkust.edu.tw
**Corresponding author: e-mail: cfyang@nuk.edu.tw
https://doi.org/10.18494/SAM4461

ISSN 0914-4935
https://myukk.org/

Previous research indicates that promoting the replacement of older, high-carbon-emitting vehicles and motorcycles with electric vehicles[1,2] and motorcycles[3,4] based on green energy is crucial for enhancing air quality and mitigating total carbon emissions.[5] The aim of our research is to develop a new electric motorcycle that is more cost-effective and reliable than existing market products. This will increase the likelihood of ordinary people purchasing an electric motorcycle over a traditional fuel-powered one, ultimately supporting the growth of the green energy industry and helping to achieve the objectives of energy conservation and carbon reduction.

The frame of a motorcycle serves as its fundamental structure, supporting the weight of all components and the rider during operation. The frame must also withstand external forces resulting from poor road conditions. The loads from the road surface, transmitted through the front and rear wheels and suspension system, are the primary factors contributing to deformation of the frame structure.[6,7] As a result, a frame structure must possess sufficient rigidity and elasticity to endure these external loads and prevent permanent deformation that could impact the stability of other frame components. The reduced handling performance of a motorcycle or vehicle could pose a significant safety risk to the rider. If the frame structure is poorly designed or the rigidity of the materials used deteriorates due to daily use, the frame's load capacity will significantly decrease, leading to a reduction in the performance of the vehicle or motorcycle.

ANSYS software has been utilized for finite element method (FEM) analysis to investigate the bending moment stiffness on the frame of an electric motorcycle.[8] ANSYS FEM software can also be used to conduct modal analyses to identify the frame's natural frequencies and modal shapes in both vehicles and motorcycles. In 2015, Marzuki *et al.* utilized ANSYS Design Modeler to create a geometric model of a sports car frame and ANSYS to analyze its natural vibration modes. Their results were consistent with the observed characteristics of the geometric model.[9,10] The simulation results confirmed that the natural vibration levels of the sports car frame did not pose any safety risks to the driver. In 2017, Ahmed *et al.* employed SolidWorks to develop a model of a solar car frame and subsequently used ANSYS 13.0 FEM software to analyze and obtain load, stress, and strain data before and after collisions.[11] These and other studies indicate that FEM is a reliable numerical calculation method and that the FEM analyses of electric motorcycle frames can effectively be used to correct design flaws.[12–14]

For example, Rodriguez *et al.* utilized SolidWorks drawing software to create a 3D model of a two-wheeled motorcycle, which was then imported into FEM software to generate an analysis model.[15] They also analyzed the drive system and telescopic mechanism models, and the results were utilized as a reference for dynamic design. These results serve as a basis for dynamic responses and computational analyses of relevant motorcycles and vehicles.[16,17] To conduct FEM software analyses of electric motorcycle frames, researchers must first have a thorough understanding of the software and its analysis process, as well as an in-depth comprehension of mechanical characteristics and FEM theory. This can be a significant challenge for ordinary designers. Therefore, the development of specialized models for FEM analyses of the frames of newly designed electric motorcycles has become an urgent need for motorcycle companies to improve their independent research and development capabilities.

Two methods were previously used to determine the effects of various loads on the full-load, modal, and fatigue life of an electric motorcycle frame. In the past, the predominant approach for detecting stress on the primary structure of electric motorcycles involved utilizing conventional sensors such as rotation sensors and pedal force sensors.[18,19] However, this method was time-consuming and inconvenient to implement. An alternative approach involved employing numerical analysis software for simulation purposes. In this study, we focused on using simulation analysis to investigate the characteristics of an electric motorcycle's frame, predict potential defects in its structure, and provide directions for its modification to obtain a frame with better mechanical properties. The analysis was conducted on an electric motorcycle with a prototype frame structure that was smaller and lighter than that of conventional electric motorcycles using ANSYS FEM software. We mainly simulated the frame deformation under different load conditions and identified the weak areas in the frame structure of the newly designed electric motorcycle that needed strengthening. To simplify the mechanical models, we specified the coordinate systems of the geometric models. Our main objective was to analyze the electric motorcycle's frame using simulation analysis technology to predict structural defects and guide modifications towards a frame with improved mechanical properties. The force model of the prototype frame structure was analyzed using ANSYS FEM software. FEM software is also used to analyze the stress mode, including chassis rigidity, strength analysis, and chassis structural simulation, to explore the stress deformation of the frame under load conditions. This enabled the automatic creation of FEM models for the electric motorcycle frame, reducing the technical difficulty and workload of FEM preprocessing. The investigated system can automatically detect the model type based on the analysis type and check for errors in the model geometry. It can also select appropriate elements for analysis and allow users to change the element type via a program. The ANSYS simulation process is feasible and accurate, as confirmed by comparing its results with those of traditional manual analysis.

2. Simulation Process and Use of Parameters

The frame of an electric motorcycle is the primary structure that bears external forces. During operation, the frame is subjected to irregular and repeated loads, leading to fatigue damage. Therefore, designing the frame structure is a crucial step in developing an electric motorcycle, with the primary considerations being its rigidity and strength.[17] We first used SolidWorks, a CAD computer-aided design software package, to create a 3D model of the frame with a 1:1 scale. After determining the appropriate meshes and nodes, a comprehensive stress analysis was performed to confirm that there was no interference between the different parameters in the design. Next, we imported the designed frame into FEM ANSYS software to verify the stress distribution. We conducted a thorough and systematic analysis to determine whether the frame for the electric motorcycle met our expectations regarding its strength. To expedite the analysis process, we appropriately simplified the model without compromising its accuracy. The principles of simplification used were carefully selected to ensure that the analysis results remained unaffected. The appropriate simplification principles are as follows.

(a) Only the frame structure of the motorcycle is taken into consideration, and any structural geometry that does not affect the analysis results is excluded.
(b) The welding effect of the frame is not taken into account during the simulation process.

The simplified geometric frame model for the electric motorcycle is illustrated in Fig. 1. During the optimization process, a crucial step involves transforming the original physical problem into a standard mathematical model. This process can be broadly categorized into the following three steps: (1) selecting the design variables, (2) defining the constraints, and (3) defining the objective function. In this study, A36 structural steel was selected as the material for the electric motorcycle frame. The material parameters of this steel are presented in Table 1, while Table 2 outlines the boundary conditions utilized in the initial analysis of the frame. The von Mises yield criterion was employed to calculate the stress of the frame, and the corresponding calculation equation is known as the von Mises stress equation.[20] If the stress components of the von Mises pressure are considered, the equation is

$$\sigma^2_{\text{von-Mises}} = (\sigma_x + \sigma_y)^2 - 3(\sigma_x\sigma_y - \sigma^2_{xy})^2, \tag{1}$$

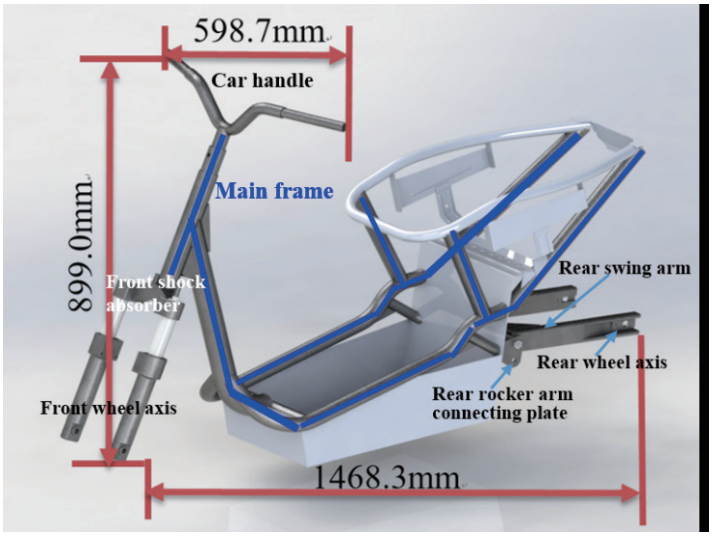

Fig. 1. (Color online) Schematic diagram of frame for a newly designed electric motorcycle.

Table 1
Parameters of A36 structural steel.

	Value
Density (kg/m^3)	7850
Tensile strength (MPa)	400
Yield strength (MPa)	250
Young's coefficient (GPa)	200
Shear modulus (GPa)	76.92
Bulk modulus (GPa)	166.67
Poisson's ratio	0.3

Table 2
Boundary conditions of the preliminary analysis.

Position	Boundary condition
Seat tube	Load 500 N
Rear wheel	Rear axle restrained
Front wheel	Front axle restrained

where σ_x, σ_y, and σ_z are the principal stresses in three directions at the points considered in the structure. If only the performance of the principal stress is considered, the equation is

$$\sigma^2_{\text{von-Mises}} = 1/2[(\sigma_x - \sigma_y)^2 + (\sigma_y - \sigma_z)^2 + (\sigma_z - \sigma_x)^2]. \quad (2)$$

In this paper, equivalent stress was used as a metric to compare the analysis results. The ANSYS Workbench FEM software employed different colors to represent the stress values, which aided in the subsequent observation and discussion of the results.

For this analysis model, a combination of triangular and tetrahedral meshes were utilized, with a mesh size of 3 mm. The mesh comprised 2161306 nodes and 1112357 elements. Mesh refinements were applied to the connections between the seat tube and the main frame, as well as the connections between the main frame and the reinforcement tubes, as shown in Figs. 2(a) and 2(b), respectively. Table 3 summarizes the numbers of mesh nodes and grid elements investigated in this study.

3. Simulation Results and Discussion

The full-load strength analysis aimed to simulate the frame's behavior under various forces, as shown in Fig. 3. The fixed support was located at point A, while forces of 500, 50, 50, and 200 N were applied at points B, C, D, and E, respectively. The analysis results are presented in Table 4, while the locations of maximum stress, maximum deformation, and maximum strain (rear axle) are illustrated in Figs. 4(a)–4(c), respectively. As depicted in these figures, the position with the maximum von Mises stress was located at the rear axle, whereas the position with the

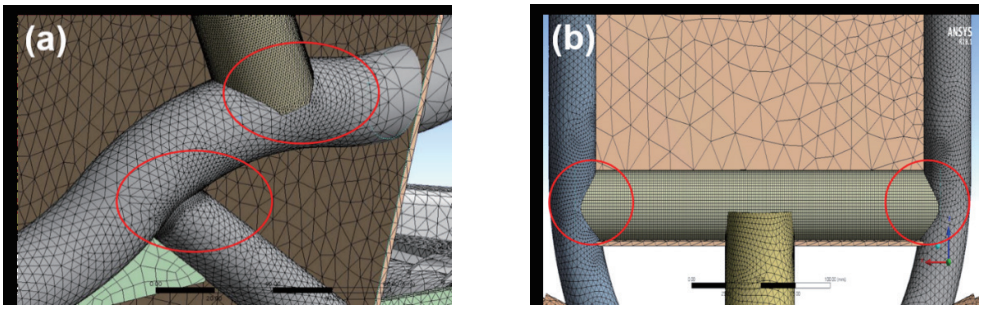

Fig. 2. (Color online) Densified area of mesh refinement at connections (a) between seat tube and main frame and (b) between the main frame and the reinforcement tubes.

Table 3
Description of grid.

Complete frame		Number used for frame stiffness analysis
Grid elements	1112357	360695
Mesh nodes	2161306	525445
Grid type	Tet10	

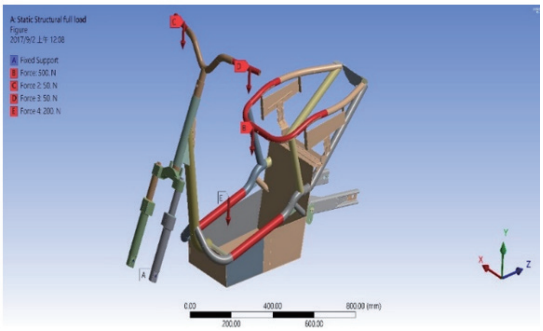

Fig. 3. (Color online) Boundary conditions in full-load analyses.

Table 4
Results of the full-load analyses.

Maximum stress (MPa)	Maximum deformation (mm)	Maximum strain (mm/mm)
119.54	0.62	0.00076
Rear axle	Handlebars	Head tube

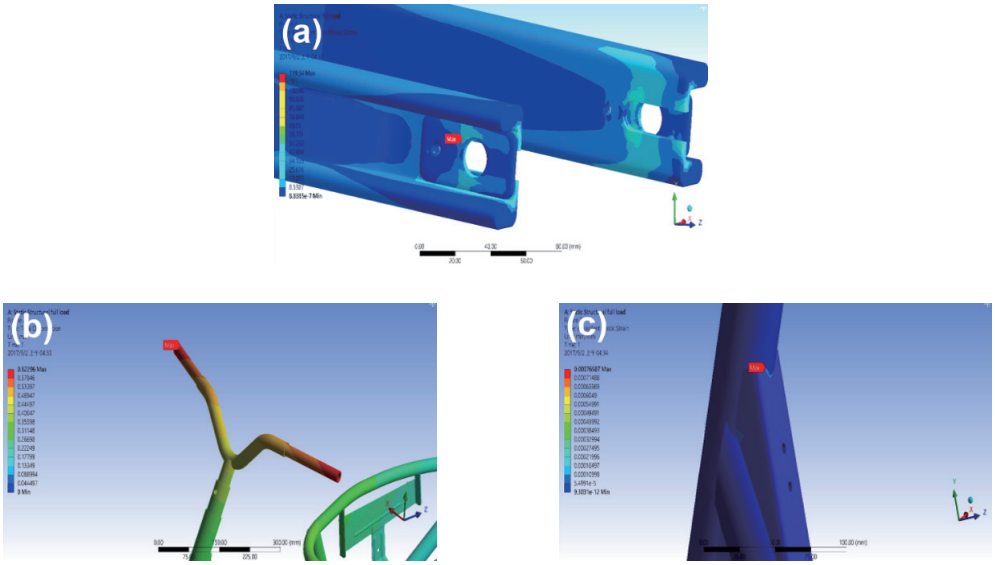

Fig. 4. (Color online) Results of full-load von Mises stress analysis: (a) position (rear axle) with the maximum stress, (b) position (handlebars) with the maximum deformation, and (c) position (head tube) with the maximum strain.

maximum deformation was located at the two handlebars. Furthermore, the maximum stress was located at the head tube. The maximum stress, maximum deformation, and maximum strain were 119.54 MPa, 0.62 mm, and 0.00076 mm/mm, respectively. From the stress distribution obtained by the analysis, it is evident that the stressed area is dispersed and not concentrated in a particular region. Moreover, the FEM analysis indicates that the maximum stress values of the newly designed electric motorcycle frame are within the yield range of the material (250 MPa). Nevertheless, 119.54 MPa is much less than the allowable value of 250 MPa. These simulation results indicate that the designed frame is safe to use under full load.

Vibrations and dynamics are critical issues in mechanical, structural, and civil engineering. Neglecting to discuss the structures or components of designed objects and not ensuring their stable dynamic conditions can result in failures caused by vibrations, which can, in severe cases, lead to their destruction, such as the collapse of a bridge. Therefore, simulation is crucial for determining the dynamic response of the structure of a newly designed object. By constructing a geometric model and conducting simulation and analysis, values of parameters that enhance the stability of the structural dynamic performance can be obtained before the actual production or fabrication of an object. Several key points must be clarified when studying the dynamic performance of structures. Firstly, an object can have multiple vibration modes, each with a different modal frequency. Secondly, the lowest-frequency mode is referred to as the first mode, and vibrations in different directions are referred to as mode shapes, each having a unique natural frequency. Lastly, vibration modes are inherent bulk properties of elastic objects.

Modal analyses enable us to understand the main mode characteristics of different orders within a certain susceptible frequency range and predict the actual vibration response of an object's structure under various external or internal vibration sources within these frequencies. These analysis results help confirm the mode shapes of different vibrations. Specifically, the modal analyses in this study aimed to identify the natural frequencies and modes (mode shape) of the frame for an electric motorcycle, including the natural frequency of the frame structure and the vibration frequencies after adding loads to the structure. The key frequency ranges can serve as reference points for designing the electric motorcycle frame. In this modal analysis, only the first- through sixth-order frequencies were considered, as the frame is subject to larger amplitude vibrations at lower frequencies. This design approach ensures that the electric motorcycle frame can withstand severe deformations under these conditions. Therefore, special attention should be given to areas with high amplitude, and reinforcement should be considered if necessary. The analyzed modal diagram provides insight into the mode shape of each frequency. This allows the identification of frequencies and structural deformation tendencies that resonate with the moving parts, serving as a reference for reinforcing the frame of the electric motorcycle.

To conduct natural vibration modal analysis on the designed electric motorcycle frame, the front and rear axles were restrained with no load, and the results obtained for the boundary conditions are summarized in Table 5, which also includes the analysis frequency and maximum displacement for each vibration mode. As the vibration mode increased from the first to the sixth order, the frequency increased from 48.313 to 98.743 Hz, whereas the maximum displacement

Table 5
Results of the natural vibration modes.

Mode	Frequency (Hz)	Maximum displacement (mm)
First order	48.313	16.731
Second order	54.115	20.723
Third order	66.124	21.125
Fourth order	70.625	11.301
Fifth order	92.768	42.107
Sixth order	98.743	15.211

did not show any consistent trend with increasing order number. Figure 5 shows the locations of the designed electric motorcycle frame with the modal frequencies and maximum deformations across the six vibration orders. Analysis of the state responses and deformation results for the six natural vibration modes revealed that the maximum deformation of 42.107 mm occurred at the fifth order, which resonated at a frequency of 92.768 Hz.

Figure 3 shows the boundary conditions for the vibration modal analyses after applying counterweight loads. For the full-load condition, both the front and rear axles were restrained. The exterior of the mode shape can indicate the deformation tendencies of the designed electric motorcycle frame at specific natural resonant frequencies. If the rigidity of the frame material requires increasing, these weaker areas can be reinforced accordingly. Figure 6 illustrates the positions of the modal frequencies and maximum displacements for the six vibration orders of the designed electric motorcycle frame under full load. Table 6 and Fig. 6 show the vibration modes and maximum displacements (deformations) for the first through sixth orders after adding the counterweight loads. Figure 6 reveals that the obtained mode shapes are primarily bending and torsional vibrations. Note that the positions of the six vibration modes are consistent with those in Fig. 5.

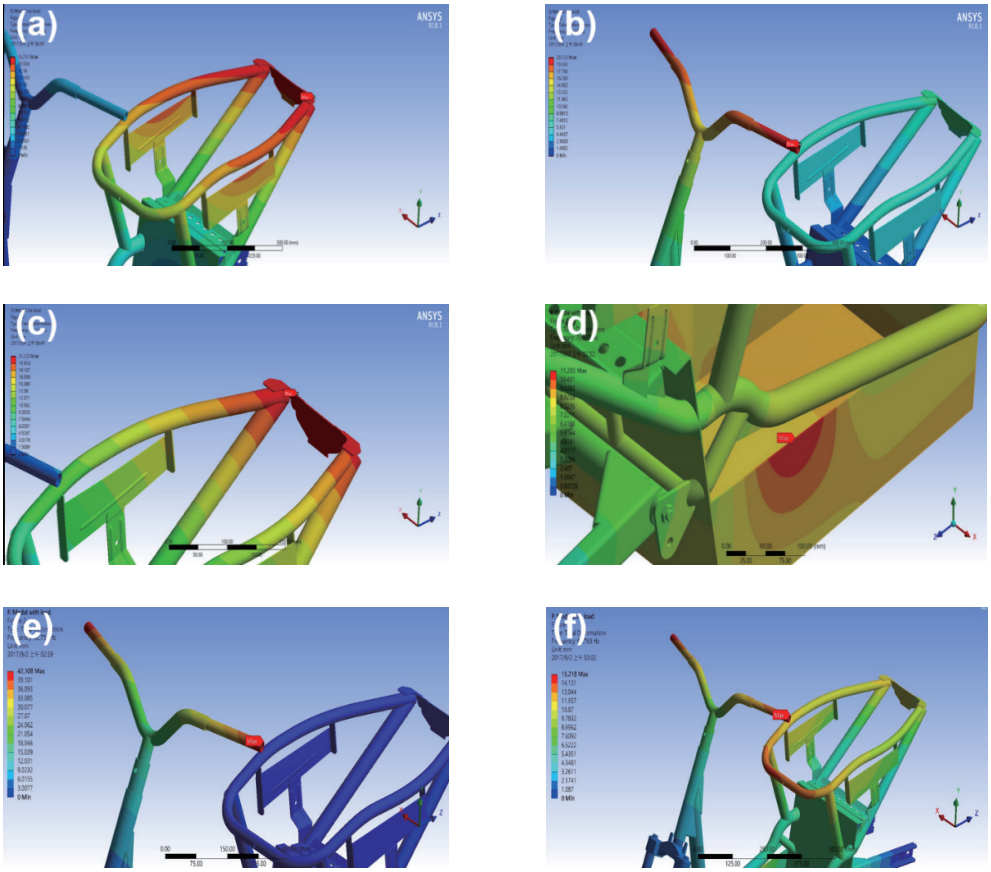

Fig. 5. (Color online) Locations of the six vibration modes: (a) first-order vibration mode (48.313 Hz), (b) second-order vibration mode (54.115 Hz), (c) third-order vibration mode (66.124 Hz), (d) fourth-order vibration mode (70.625 Hz), (e) fifth-order vibration mode (92.751 Hz), and (f) sixth-order vibration mode (98.743 Hz).

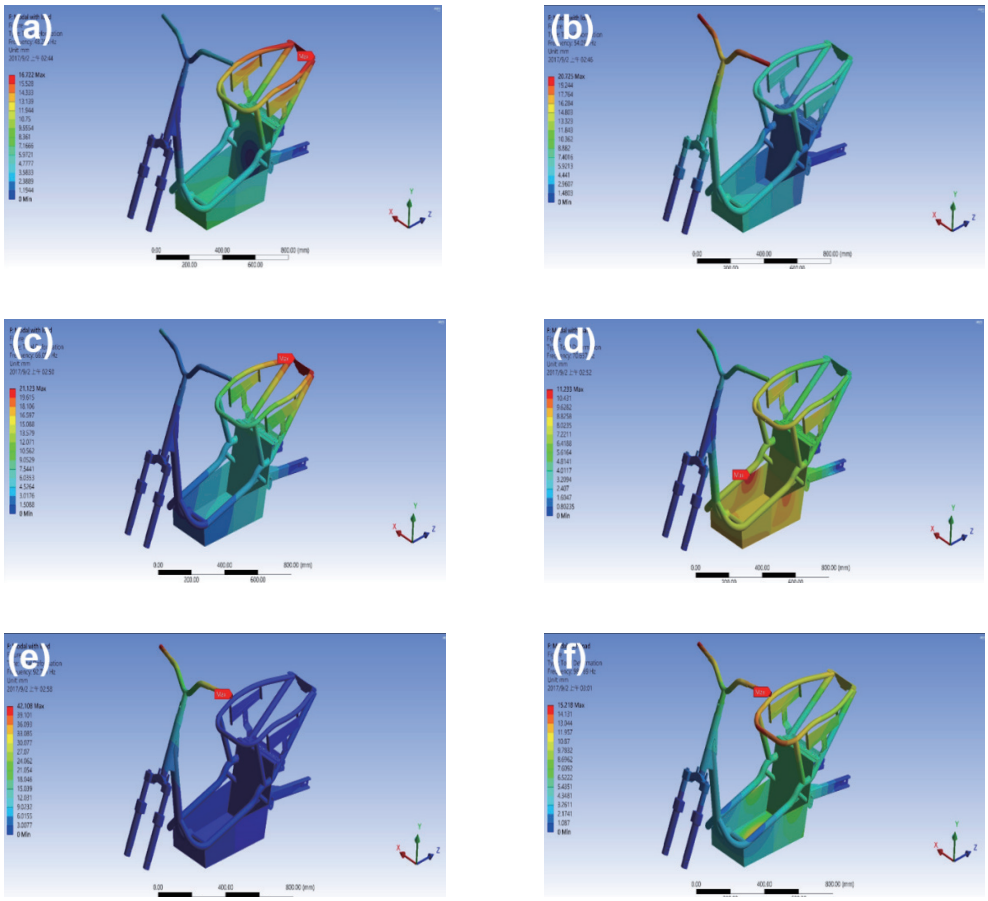

Fig. 6. (Color online) Positions of the different vibration modes after applying counterweight loads: (a) first-order vibration mode at 48.266 Hz, (b) second-order vibration mode at 54.098 Hz, (c) third-order vibration mode at 66.099 Hz, (d) fourth-order vibration mode at 70.637 Hz, (e) fifth-order vibration mode at 92.751 Hz, and (f) sixth-order vibration mode at 98.769 Hz.

Table 6
Analysis results of the different vibration modes after applying counterweight loads.

Mode	Frequency (Hz)	Maximum displacement (mm)
First order	48.266	16.722
Second order	54.098	20.725
Third order	66.099	21.123
Fourth order	70.637	11.233
Fifth order	92.751	42.108
Sixth order	98.769	15.218

Tables 5 and 6 demonstrate that the discrepancies in the modal frequency and maximum displacement between the natural vibration and the vibration after adding counterweight loads obtained via FEM software are negligible, or even nonexistent, for each order. For example, according to Table 6, the designed frame with full load experienced a maximum displacement of 42.108 mm at the fifth order with a resonant frequency of 92.751 Hz. Notably, both the maximum

displacement and resonant frequency are similar to those obtained with no load in Table 5. These findings indicate that the designed electric motorcycle frame retains its stable mechanical properties even after adding the loads in Fig. 3. Hence, the FEM model utilized in this study is reliable for further analysis of the designed electric motorcycle frame. The outcomes indicate that the frame can withstand the full loads depicted in Fig. 3. Nonetheless, caution should be exercised when adding other equipment or items to the frame or choosing a drum motor to propel the electric motorcycle as it may result in vibrations at a frequency of ~92.75 Hz, leading to substantial displacement and resonance of the frame structure.

Fatigue is caused by repeated loading and is typically categorized into two types: high-cycle fatigue and low-cycle fatigue. In this study, we used a fatigue model employing stress-based theory, which is suitable for analyzing high-cycle fatigue. When the maximum and minimum stress levels remain constant, a fatigue is referred to as a constant amplitude load. We employed this load model to conduct our fatigue analysis. In real-world scenarios, many crucial or core structural positions of a frame experience multiaxial loads. This means that a critical joint or position will bear more than one type of stress, or the direction of principal stress will change over time due to variations in the loads from the roads. To account for this, a fatigue tool is used to perform fatigue life calculations under principal stress states and multiaxial conditions. Certain components, such as joints and crankshaft connecting rods, are anticipated to be subjected to high cyclic loads throughout their lifespan. To design tests and perform finite fatigue life analyses on these components, the "factor safety" method is commonly employed. This method measures how much stronger a system is compared with the required strength for various intended loads. In other words, the load cycles can be compared with the fatigue or endurance limit criteria. We conducted a fatigue life analysis using the full load as the boundary conditions, and the safety factor was simulated and analyzed, the results of which are shown in Fig. 7. The results indicate that the minimum safety factor of ~4.8, which is significantly higher than the value of 1.9 reported in Ref. 4, occurred at the rear axle. The safety factors for the other components of the designed electric motorcycle frame were all above 10. These results demonstrate that the frame structure is capable of withstanding a large number of usage cycles.

In an S–N curve, the *x*-axis represents the number of cycles of applied stress that causes the material to deform, usually expressed in logarithmic coordinates, and the *y*-axis represents the magnitude of the stress. If the stress is below a certain value in the S–N curve, the material will

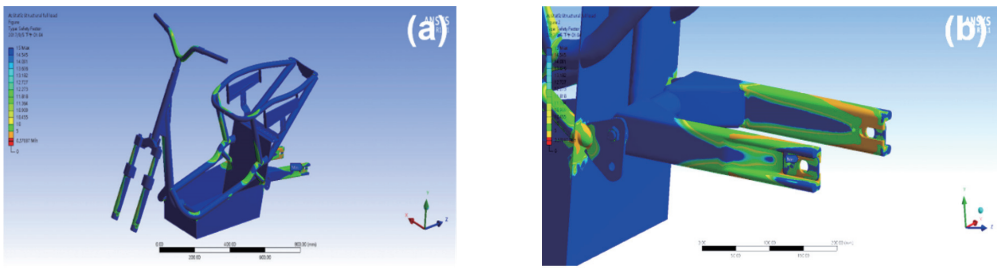

Fig. 7. (Color online) (a) Results of analyses of the safety factor of the designed electric motorcycle frame under load condition. (b) Location where the safety factor is minimum.

not experience fatigue damage even if the number of stress cycles is increased. This value is known as the fatigue limit of the material. We analyzed the life S–N curve to determine how many cycles the designed electric motorcycle frame can withstand for a given stress range. The fatigue tool was used to determine the number of cycles for forces in the range from 50 to 200% of full load. As shown in Fig. 8, the designed electric motorcycle frame can withstand 9.41×10^3 cycles when the force is 50% of full load and 186 cycles when the force is 200% of full load. Murakami *et al.* proposed a method to predict the fatigue limit and fatigue life of materials with scatter and defects.[21] They identified three different regions in the S–N curve: the Basquin model region, the Palmgren model region, and the Stromeyer model region, as illustrated in Fig. 8.

(a) In the Basquin model region, there is a logarithmic relationship between the number of cycles to failure (N) and the applied stress amplitude. As the stress amplitude increases, the fatigue life decreases.
(b) The Palmgren model region corresponds to a flat plateau in the S–N curve, indicating that fatigue failure will not occur if the applied stress is below a certain level.
(c) The Stromeyer model region represents the region below which no fatigue failure occurs.

As shown in Fig. 8, our results are consistent with the Basquin and Palmgren models when the load exceeds 45% of full load. However, when the load ratio is less than 0.45, the Stromeyer model is not followed, making it challenging to predict the fatigue life using the Stromeyer model. Additionally, the fitting line between the Stromeyer model and the modified Miner's rule has been observed in Fig. 8. Murakami *et al.* discovered that the modified Miner's rule, the Palmgren–Miner rule, and Miner's rule are not suitable for fitting this type of curve because it is challenging to accurately evaluate fatigue damage for stress cycles with an amplitude lower than the fatigue limit.[21] However, our simulation results show that even when the load is below the fatigue limit, variations in the fatigue life can still be obtained.

The biaxiality ratio is defined as the smaller principal stress divided by the larger one. Analyzing the biaxial stress contour model is useful for identifying the local stress state. The

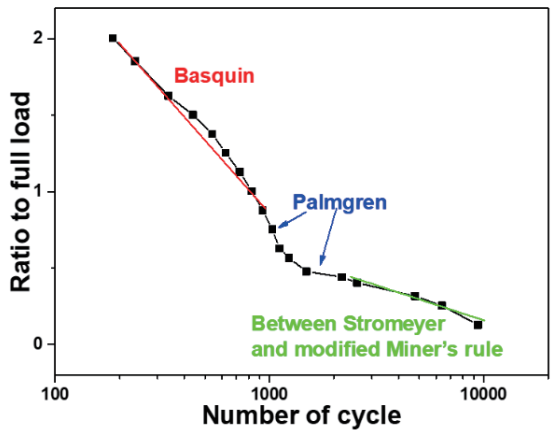

Fig. 8. (Color online) Life S–N curve.

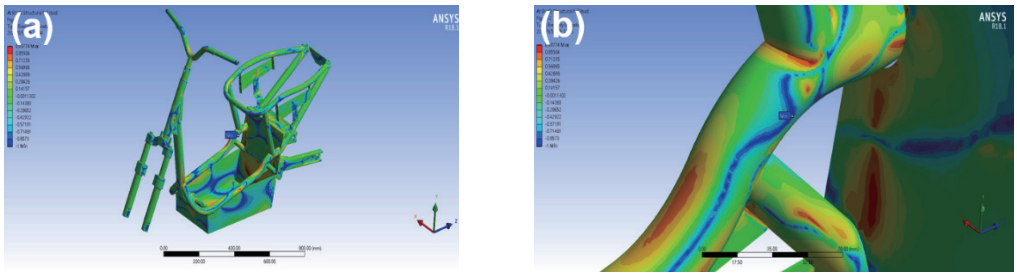

Fig. 9. (Color online) (a) Force distribution diagram of double axles of frame and (b) position with the maximum shear force.

scale is 0 for an area under uniaxial stress, 1 for an area under biaxial stress, and −1 for an area under pure shear stress. After conducting the aforementioned analyses, we determined the force distribution diagram for the double axles of the designed electric motorcycle frame and the location of the maximum shear force, which are depicted in Fig. 9. The area with the highest shear force is at the junction of the main frame and the seat tube. Consequently, the structural integrity of this specific area should be a priority for designers. The fatigue analyses aim to examine the stress distribution and cycle life of the mounting base of the shock absorber in the designed electric motorcycle frame under an external force. Through the applications of various fatigue correction theories and modifications to the model geometry, the designed electric motorcycle frame has been improved by the two approaches to achieve the desired goals.

4. Conclusions

In this study, we analyzed the full-load, modal, and fatigue life of an electric motorcycle frame by utilizing a combination of triangular and tetrahedral meshes with a mesh size of 3 mm consisting of 2161306 nodes and 1112357 elements. The discrepancies in the modal frequency and maximum displacement between the natural vibration and the vibration after adding counterweight loads were found by simulation with FEM software to be negligible for each order, and the designed frame with full load experienced a maximum displacement of 42.108 mm at the fifth order with a resonant frequency of 92.751 Hz. The full-load strength analysis revealed that the highest stress of 119.54 MPa was located at the rear axle, the maximum deformation of 0.62 mm was at the two handlebars, and the maximum strain of 0.00076 mm/mm was at the head tube. For the natural vibration frequencies and modes with full load, the vibration modes increased from the first to sixth order; the frequency range increased from 48.313 to 98.743 Hz and the maximum displacement of 42.107 mm appeared for the fifth order. Under forces of 50 and 200% of full load, the designed electric motorcycle frame could withstand 9.41×10^3 and 186 cycles, respectively. Analyzing the full-load, modal, and fatigue life of an electric motorcycle frame using FEM software provides valuable insights into its structural integrity, performance under different conditions, and expected lifespan. This comprehensive analysis aids in optimizing the design, enhancing durability, and ensuring the safe and reliable operation of the electric motorcycle.

Acknowledgments

This work was supported by project Nos. MOST 109-2221-E-390-023, MOST 110-2622-E-390-002, and MOST 110-2221-E-390-020.

References

1 P. Nigam, D. Sahu, and A. M. Bisen: Int. J. Eng. Res. Technol. **9** (2020) 527.
2 W. Sumbodo, R. Wahyudi, Setiadi, F. A. Kriswanto, and Budiman: J. Appl. Sci. Eng. **19** (2021) 948.
3 S. Rege, C. Khatri, M. Nandedkar, and N. Wagh: Int. J. Innov. Res. Sci. Eng. Technol. **6** (2017) 19500.
4 P. Jeyapandiarajan, G. Kalaiarassan, J. Joel, S. Rutwesh, F. T. Fastin, and B. Aditya: Proc. Materials Today **5** (2018) 13563–13573.
5 J. R. Chou and S. W. Hsiao: Int. J. Ind. Ergon. **35** (2005) 1047.
6 G. M. Angle II and W. W. Huebsch: Aerodynamic Drag Reduction of a Racing Motorcycle through Vortex Generation (Pennsylvania, SAE International in United States, 2002).
7 N. Petrone and M. Saraceni: Frattura ed Integrità Strutturale **8** (2014) 226.
8 H. M. Dai, B. H. Chen, C. M. Hsu, and C. F. Yang: Sens. Mater. **34** (2022) 1732.
9 M. A. B. Marzuki, M. A. A. Bakar, and M. F. M. Azmi: Int. J. Inf. Syst. Eng. **3** (2015) 54.
10 S. I. Cahyono, M. Anwar, K. Diharjo, T. Triyono, A. Hapid, and S. Kaleg: Proc. AIP Conf. **1788** (2017) 030084.
11 M. Y. Ahmed, A. Nihar, M. Nayeemuddin, M. Ahmed, and Abdullah: J. Sci. Res. Sci. Eng. Technol. **3** (2017) 373.
12 D. Chindamo, M. Gadola, D. Armellin, and F. Marchesin: Appl. Sci. **7** (2017) 1220.
13 R. Kharul, S. Balakrishnan, D. Karedla, and S. S. You: SAE Int. J. Mater. Manuf. **3** (2010) 541.
14 M. Vignesh, K. Arumugam, S. Vinoth, and S. Hariharan: Int. J. Eng. Sci. Inven. **8** (2019) 8.
15 J. E. Rodriguez, A. L. Medaglia, and J. P. Casas: Proc. 2005 IEEE Design Symp. Systems and Information Engineering (2005) 277–285.
16 C. A. Manrique-Escobar, C. M. Pappalardo, and D. Guida: Machines **9** (2021) 245.
17 G. E. Roe and T. E. Thorpe: SAE Int. J. Passeng. Cars **98** (1989) 1319.
18 Advice about electric bikes: https://www.gazellebikes.com/en-gb/advice/electric-bike/sensors (accessed March 2023).
19 Classification: https://www.ezb2b.com/eng/v25-motorcycle-frame-body (accessed April 2023).
20 W. A. Siswanto and T. W. Besar Riyadi: Mater. Sci. Forum **961** (2019) 137.
21 Y. Murakami, T. Takagi, K. Wada, and H. Matsunaga: Int. J. Fatigue **146** (2021) 106138.